Structure, Miscibility, and Rheological Characteristics of β-Casein–Monoglyceride Mixed Films at the Air–Water Interface

Juan M. Rodríguez Patino,* Mª. Rosario Rodríguez Niño, and
Cecilio Carrera Sánchez

Departamento de Ingeniería Química, Facultad de Química, Universidad de Sevilla, c/o Professor
García González s/núm, 41012-Seville, Spain

In this work we have used different and complementary interfacial techniques (surface film balance, Brewster angle microscopy, and interfacial dilatational rheology) to analyze the static (structure, morphology, reflectivity, miscibility, and interactions) and dynamic characteristics (surface dilatational properties) of β-casein and monoglyceride (monopalmitin and monoolein) mixed films spread on the air–water interface. The static and dynamic characteristics of the mixed films depend on the interfacial composition and the surface pressure. At higher surface pressures, collapsed β-casein residues may be displaced from the interface by monoglyceride molecules with important repercussions on the interfacial characteristics of the mixed films. From the frequency dependence of the surface dilatational properties, we have elucidated the relationships between interfacial dilatational rheology and changes in molecular structure, interactions, miscibility, and relaxation phenomena in protein–monoglyceride mixed films.

KEYWORDS: Interfacial dynamic properties; monolayer structure; Interfacial rheology; air–water interface; food emulsifiers; food dispersions; protein–monoglyceride mixed films

INTRODUCTION

The stability and mechanical properties of food-dispersed systems (emulsions and foams) depend on the way in which the constituent particles and macromolecules adsorb and interact at fluid–fluid interfaces (*1*). To stabilize food emulsions and foams, emulsifiers (lipids, phospholipids, and proteins) must be adsorbed at the interface, so they can form a film around droplets or bubbles, respectively. The optimum use of emulsifiers depends on the knowledge of their interfacial physicochemical characteristics—such as surface activity, structure, stability, interfacial rheological properties, etc.—and the kinetics of the film formation at fluid–fluid interfaces (*1, 2*). Nonequilibrium processes occurring in systems containing fluid–fluid interfaces with a surfactant present are of great practical significance. Among many food-dispersed systems, they include important technological operations such as emulsification, emulsion coalescence and break-up, foaming froth flotation, extraction, distillation, adsorption, heterogeneous catalysis, electrochemical reactions, detergency, complex coating process, oil recovery, natural phenomena, etc. (*3–7*).

Emulsifiers used in commercial food formulations typically consist of a mixture of surface-active derivatives because they can be produced at a relatively lower cost than pure emulsifiers. In addition, in many emulsifier applications, mixtures of different emulsifiers (mainly polar lipids and proteins) often exhibit properties superior to those of the individual emulsifier alone due to synergistic interactions between emulsifier molecules. In previous works with mono- and diglycerides (*8–10*) or mixtures of monoglycerides and milk proteins (*11, 12*) we observed that when molecules of both emulsifiers were spread at the air–water interface they were more expanded or packed more closely together than when either emulsifier was present alone, indicating some form of association. Interactions between molecules of emulsifiers could affect not only film structure and morphology (*13–15*) but also the relaxation phenomena in mixed films (*16, 17*). Information about these phenomena would be very helpful in the prediction of optimized formulations for food foams and emulsions. So far, there are only a few experimental results available on surface rheological behavior of mixed surfactants adsorbed at fluid–fluid interfaces (*5, 18–20*). As far as we know, the same applies for studies on interfacial rheological properties of oil-soluble emulsifiers (monoglycerides and phospholipids) in combination with proteins spread at the air–water interface, although in practice mixtures of these emulsifiers are usually used in order to reach an optimal effect in food formulations (*1, 18–21*).

The aim of this contribution was to analyze the static (structure, morphology, relative reflectivity, and interactions) and surface dilatational properties of mixed food emulsifiers (β-casein and monoglycerides) at the air–water interface. In this work we have used for the first time, a unique device that incorporates different interfacial techniques, such as surface film balance, Brewster angle microscopy, and interfacial dilatational

* To whom all correspondence should be addressed. Telephone: +34 95 4557183. Fax: +34 95 4557134. E-mail: jmrodri@us.es.

Properties of β-Casein–Monoglyceride Mixed Films

J. Agric. Food Chem., Vol. 51, No. 1, 2003 **113**

rheology. Monolayers at the air−water interface are interesting systems for studying two-dimensional structures of amphiphilic substances. In addition, insoluble monolayers at the air−water interface have a wide range of applications including models for dispersed systems (emulsions and foams). In this work we have observed that there exist close relationships between surface dilatational properties and structural characteristics and relaxation phenomena (*17*) in β-casein−monoglyceride mixed films. The surface dilatational properties of protein−monoglyceride systems are of interest due to their importance in relation to food dispersion formation and stability (*1, 4, 7, 18, 19, 21*).

EXPERIMENTAL PROCEDURES

Chemicals. Synthetic 1-monohexadecanoyl-*rac*-glycerol (monopalmitin, DIMODAN PA 90) and 1-mono(*cis*-9-octadecanoyl)glycerol (monoolein, RYLO MG 19) were supplied by Danisco Ingredients with over 95−98% purity. β-Casein (99% pure) was supplied and purified from bulk milk from the Hannah Research Institute, Ayr, Scotland. Samples for interfacial characteristics of β-casein films were prepared with Milli-Q ultrapure water and were buffered at pH 7. To form the surface film, monoglyceride was spread in the form of a solution, using hexane:ethanol (9:1, v:v) as a spreading solvent. Analytical grade hexane (Merck, 99%) and ethanol (Merck, >99.8%) were used. The water used as subphase was purified by means of a Millipore filtration device (Milli-Q). A commercial buffer solution called trizma ((CH$_2$-OH)$_3$CNH$_2$/(CH$_2$OH)$_3$CNH$_3$Cl) was used to achieve pH 7. All these products were supplied by Sigma (>99.5%). Ionic strength was 0.05 M in all the experiments.

Surface Film Balance. Measurements of surface pressure (π)−area (*A*) isotherms of β-casein−monoglyceride mixed films at the air−water interface were performed on a fully automated Wilhelmy-type film balance. The method has been described previously for pure (*22, 23*) and mixed components (*13, 14*). Before each measurement, the film balance was calibrated at 20 °C. Mixtures of particular mass ratios−ranging between 0 and 1, expressed as the mass fraction of monoglyceride in the mixture, *X*−were studied. Aliquots of aqueous solutions of β-casein (0.1543 mg/mL) at pH 7 were spread on the interface by means of a micrometric syringe. Afterward, a monoglyceride solution in the hexane/ethanol mixture was spread at different points on the β-casein film. The compression rate was 3.3 cm min^{-1}, which is the highest value for which isotherms were found to be reproducible in preliminary experiments. The π−*A* isotherm was measured at least 6 times. The reproducibility of the results was better than ±0.5 mN/m for the surface pressure and ±0.005 nm^2/molecule for the area.

Brewster Angle Microscopy (BAM). A commercial Brewster angle microscope (BAM), BAM2, manufactured by NFT (Göttingen, Germany) was used to study the morphology of the monolayer. The BAM was positioned over the film balance. Further characteristics of the device and operational conditions have been described elsewhere (*24, 25*). The measurements of surface pressure, area, and gray level as a function of time were carried out simultaneously by means of a device connecting the film balance and BAM. These measurements were performed during sinusoidal compression and expansion of the monolayer. To measure the relative reflectivity (*I*) of the film a previous camera calibration is necessary (*24, 25*). The imaging conditions were adjusted to optimize both image quality and quantitative measurement of reflectivity. Thus, generally, as the surface pressure or the protein content increased the shutter speed was also increased.

Surface Dilatational Rheology. To obtain surface rheological parameters−such as surface dilatational modulus, elastic and viscous components, and tangent of the loss angle−a modified Wilhelmy-type film balance (KSV 3000) was used as described elsewhere (*26, 27*). In this method the surface is subjected to small periodic sinusoidal compressions and expansions by means of two oscillating barriers at a given frequency (*ω*) and amplitude (Δ*A/A*) and the response of the surface pressure is monitored (π). The amplitude was maintained constant at 5%. The percentage area change was determined (*26, 27*) to be in the linear region. Surface pressure was directly measured by means of two roughened platinum plates situated in the surface between
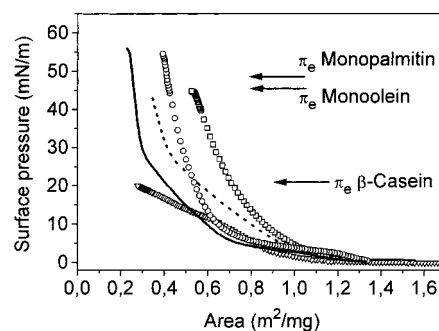

Figure 1. Surface pressure–area isotherms (compression curve) for (▽) β-casein, (○) monopalmitin, (□) monoolein, (—) β-casein–monopalmitin $X_{MP} = 0.6$, and (− − −) β-casein–monoolein at $X_{MO} = 0.6$. Temperature, 20 °C. The equilibrium surface pressures (π_e) for β-casein, monopalmitin, and monoolein are indicated by means of arrows.

the two barriers. The surface dilatational modulus derived from the change in surface pressure resulting from a small change in surface area may be described (*28*) by the eq $E = -(d\pi/d \ln A) = E_d + iE_v$.

The dilatational modulus is a complex quantity and is composed of real and imaginary parts. The real part of the dilatational modulus or storage component is the dilatational elasticity, $E_d = |E| \times \cos \theta$. The imaginary part of the dilatational modulus or loss component is the surface dilatational viscosity, $E_v = |E| \times \sin \theta$. The tangent of the loss angle is given by $\tan \theta = E_v/E_d$. If the film is purely elastic, the loss angle tangent is zero. Measurements were performed at least 3 times. The reproducibility of these results was better than 5%.

RESULTS AND DISCUSSION

Structural and Morphological Characteristics of β-Casein−Monoglyceride Mixed Films at the Air−Water Interface. Results derived from π−*A* isotherms (**Figure 1**) in the Wilhelmy-type trough are in good agreement with those obtained in the same trough with pure β-casein (*26*) and monoglycerides (*27*) and in the Langmuir-type trough with the same β-casein, monoglyceride, and β-casein−monoglyceride mixed films (*13, 14*). Briefly, the results of π−*A* isotherms confirm that β-casein monolayers at the air−water interface adopt two different structures and the collapse phase. According to Graham and Phillips (*29*), at low surface pressures β-casein molecules exist as trains with all amino acid segments located at the interface. This structure was observed at surface pressures lower than ca. 10 mN/m. At higher surface pressures, and up to the equilibrium surface pressure, amino acid segments are extended into the underlying aqueous solution and adopt the form of loops and tails. The equilibrium surface pressure (π_e) is the maximum surface pressure to which a spread monolayer may be compressed without the possibility of monolayer collapse. Different structures can be deduced for monopalmitin monolayer as a function of surface pressure (**Figure 1**). The liquid-expanded phase (LE) (at π < 5 mN/m), a first-order phase transition between liquid-condensed (LC) and liquid-expanded structures (at 5 < π < 30 mN/m), the liquid-condensed structure (at π > 30 mN/m), and, finally, the solid (S) structure near to the monolayer collapse at a surface pressure of about 53.1 mN/m were observed. In contrast with monopalmitin monolayer, monoolein monolayer presents only the liquid-expanded structure and collapses at the equilibrium surface pressure ($\pi_e \approx$ 45.7 mN/m).

β-Casein−monopalmitin and β-casein−monoolein mixed films (**Figure 1**), at a monoglyceride mass fraction of 0.6 (as an example) and at surface pressures lower than that for β-casein collapse ($\pi_C \cong$ 20.9 mN/m), adopt a structural polymorphism, as for pure components. In this region a mixed monolayer of
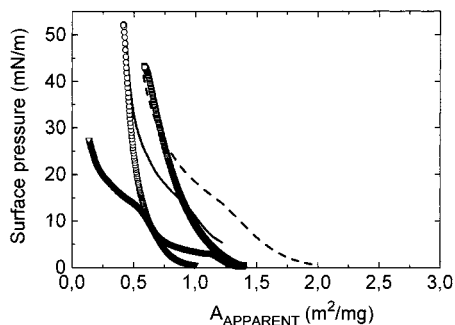
Figure 2. Surface pressure–area isotherms (compression curve) for β-casein–monoglyceride mixed monolayers. The molecular area (apparent area) was calculated on the basis that only the monoglyceride was adsorbed on the interface. Temperature, 20 °C. Key: (▽) β-casein, (○) monopalmitin, (□) monoolein, (−) β-casein–monopalmitin X_{MP} = 0.6, and (− − −) β-casein–monoolein at X_{MO} = 0.6.

monoglyceride and β-casein may exist. However, at surface pressures higher than that for β-casein collapse, the π−A isotherms for mixed monolayers were parallel to that of the monoglyceride, which demonstrates that the arrangement of the monoglyceride hydrocarbon chain in mixed monolayers is practically the same over the entire β-casein−monoglyceride ratio (*13*, *14*). That is, at higher surface pressures, collapsed β-casein residues may be displaced from the interface by monoglyceride molecules.

This conclusion is supported by the results presented in **Figure 2**. In this figure we show hypothetical π−A isotherms for a mixed monolayer at a monoglyceride mass fraction of 0.6 (as an example) calculated on the basis that only the monoglyceride is present at the air−water interface. It must be emphasized that, due to this assumption, in Figure 2 the area on the *X*-axis is not the true area per unit mass but the apparent area. For this reason the *X*-axis in **Figure 1** (for true area per unit mass) is different from that in **Figure 2** (for apparent area per unit mass). We can see that, if one assume that the mixed monolayers are dominated by monoglyceride (**Figure 2**), the π−A isotherms for monoglyceride and β-casein−monoglyceride mixed monolayers at surface pressures higher than that for β-casein collapse practically coincide (the same results were observed for all mixed films at X_{MP} > 0.2 or X_{MO} > 0.2). That is, at surface pressures higher than that for β-casein collapse, mixed monolayers behaved practically as a pure monoglyceride monolayer, at a macroscopic level. In contrast to the above data, π−A isotherms calculated again on the basis that the mixed monolayers are dominated by β-casein (data not shown) differ completely from those for pure components under all experimental conditions.

The interactions between components in mixed monolayers can be studied from the point of view of miscibility between components in the mixed monolayer (*8*, *10*). In **Figure 3** we show the molecular area (*A*) and the mean area (A_i) calculated according to the additivity rule (*30*), $A_i = A_1X_1 + A_2X_2$, where A_1 and A_2 are the molecular areas of pure components and X_1 and X_2 are the mass fractions of pure components in the mixed monolayer. The continuous lines in **Figure 3** correspond to an immiscible monolayer. For β-casein−monopalmitin mixed monolayers, the excess area was negative at every surface pressure for *X* > 0.2. That is, at surface pressures lower than that for β-casein collapse, as the film-forming components adopt a similar liquid-expanded-like structure, attractive interactions in the mixed monolayer exist. Finally, it can be seen that the collapse pressure for mixed monolayers is similar to that for monoglyceride and does not depend on the monolayer composi-
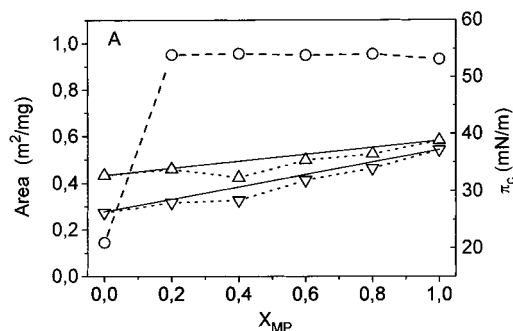

Figure 3. Molecular area at (△) 10 mN/m and (▽) 20 mN/m and (○) surface pressure at the collapse point as a function of monolayer composition for β-casein–monopalmitin mixed monolayers at 20 °C.
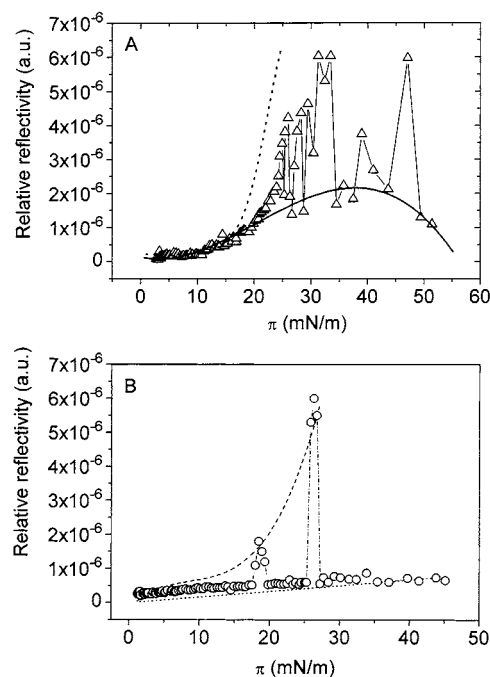

Figure 4. Relative reflectivity (arbitrary units) as a function of surface pressure during the compression of (A) β-casein–monopalmitin and (B) β-casein–monoolein mixed monolayers at 20 °C. Key: (− − −) β-casein, (−) monopalmitin, (·······) monoolein, (△) β-casein–monopalmitin mixed films at X_{MP} = 0.6, and (○) β-casein–monoolein at X_{MO} = 0.6.

tion. The practical independence of the collapse pressure on monolayer composition implies an immiscibility of the two components in the mixed monolayer (*13*, *14*) at the highest surface pressure, under the collapse conditions. β-Casein−monoolein mixed monolayers behaved in a similar way (data not shown).

Results of BAM, in particular the relative reflectivity as a function of surface pressure (**Figure 4**) and morphology (**Figure 5**) obtained with β-casein, monoglyceride, and β-casein-monoglyceride mixed films clearly show at a microscopic level the same structural characteristics as those deduced from the π−A isotherms. The domains that residues of β-casein (**Figure 5A**) and monoolein (**Figure 5B**) molecules at every surface pressure and monopalmitin with a liquid-expanded structure (image not shown) adopt at the air−water interface appeared to be of uniform reflectivity, suggesting homogeneity in thickness and film isotropy. In this region the I−π plot is a continuous line without any significant reflectivity peak (**Figure 4**). For monopalmitin monolayer circular LC domains in a homogeneous LE environment (**Figure 5C**) were observed at
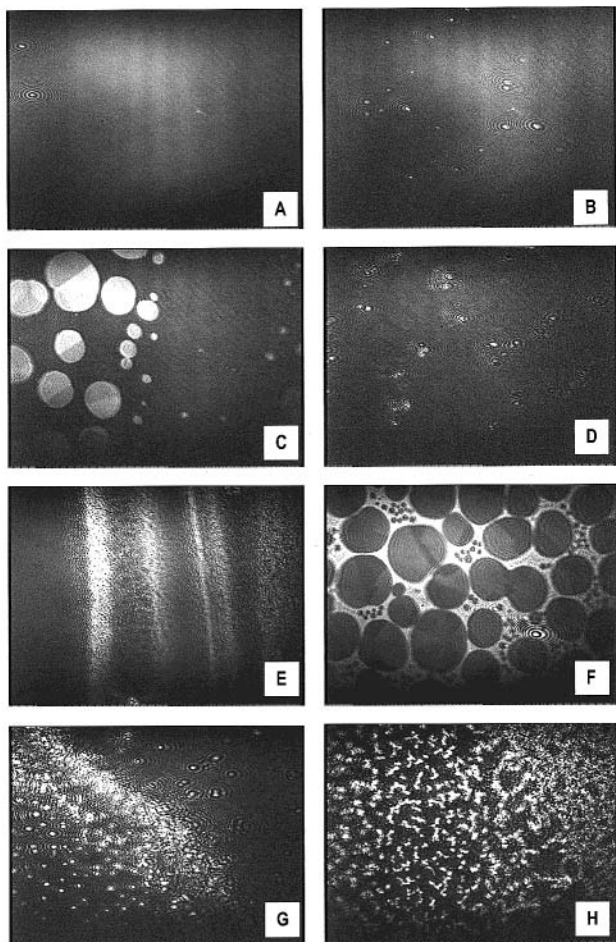
Properties of β-Casein–Monoglyceride Mixed Films

J. Agric. Food Chem., Vol. 51, No. 1, 2003   **115**

Figure 5. Visualization of β-casein, monopalmitin, monoolein, and β-casein–monoglyceride mixed films at the air–water interface. (A) β-casein (LE-like structure), π = 14 mN/m, shutter 1/125 s, (B) monoolein (LE structure), π = 30 mN/m, shutter 1/50 s, (C) monopalmitin (LE → LC transition), π = 24 mN/m, shutter 1/50 s, (D) monopalmitin (at the collapse point), π = 51 mN/m, shutter 1/125 s, (E) monopalmitin (fractures at the collapse point), π = 51.4 mN/m, shutter 1/125 s, (F) squeezing out phenomena (after the β-casein collapse) in a β-casein–monopalmitin mixed film at X_{MP} = 0.5, π = 29 mN/m, shutter 1/250 s, (G) frontier between β-casein (collapsed) and monopalmitin (solid) domains in a mixed film at X_{MP} = 0.5, π = 49 mN/m, shutter 1/250 s, and (H) squeezing out phenomena (near the collapse point) in a β-casein–monoolein mixed film at X_{MO} = 0.5, π = 29 mN/m, shutter 1/125 s.

$5 < \pi < 30$ mN/m. The LC structure was observed at $\pi > 30$ mN/m, with circular domains which grow with surface pressure. Finally, the collapse phase was observed at a surface pressure of about 53.1 mN/m, characterized by a homogeneous morphology after fusion of LC circular domains (**Figure 5D**) and the presence of monolayer fracture in different zones of the interface (**Figure 5E**). The relative intensity decreased at higher surface pressures as the monolayer collapsed (**Figure 4A**). For comparison purposes a continuous line was deduced by fitting the $I-\pi$ data, derived from different measurements for pure components (**Figure 4**).

The $I-\pi$ plot for compression of β-casein−monopalmitin mixed monolayer at 0.6 in mass fraction of monopalmitin in the mixture (as an example) is shown in **Figure 4A**. In this figure we only include the results of one measurement for clarity reasons (six $I-\pi$ plots were recorded per compression−expansion cycles with different shutter speeds for the same monolayer). These data followed essentially the same trends as

for mixtures with different mass fraction of monopalmitin. Briefly, at $\pi < 20$ mN/m, the $I-\pi$ plots were the same as for pure components. In this region, LC domains of monopalmitin existed in an environment of homogeneous LE monopalmitin and LE-like β-casein domains, during the compression. The main difference was observed in the region near the β-casein collapse (20 mN/m $< \pi < 30$ mN/m), because the relative reflectivity of the mixed film was lower than for pure β-casein. This suggests that monopalmitin is able to displace β-casein residues from the interface toward a sublayer beneath the monopalmitin monolayer. **Figure 5F** shows a characteristic squeezing out phenomenon. In fact, many LC domains of monopalmitin — the dark domains are due to monopalmitin with an LC structure — are floating over a sublayer of collapsed β-casein molecules, characterized by a completely white image with a reflectivity similar than that for pure β-casein. **Figure 5G** shows the frontier between regions of collapsed β-casein molecules and closely packed LC domains of monopalmitin near its collapse (π = 43 mN/m). The existence of these isolated spots with collapsed β-casein residues is the cause of the peaks observed in the $I-\pi$ plot.

For a β-casein−monoolein monolayer (**Figure 4B**) at 0.6 mass fraction of monoolein in the mixture and surface pressures lower than that for β-casein collapse, the I values were similar to that for β-casein or monoolein as the monoolein mass fraction approached 0 or 1, respectively. At surface pressures higher than 25 mN/m, the $I-\pi$ plots approached that for pure monoolein monolayer. However, some peaks with a relative reflectivity similar to that for a collapsed β-casein monolayer were observed. In fact, some white spots were also observed (**Figure 5H**) due to the presence of collapsed β-casein molecules. Finally, at the collapse point, the reflectivity peaks disappeared in the $I-\pi$ plot and the relative reflectivity decreased to a value close to that for pure monoolein monolayer (**Figure 4B**). This result suggests that in this region mixed monolayers were dominated by the presence of monoolein at the interface, as deduced for β-casein−monopalmitin mixed film. However, BAM images (**Figure 5**) also demonstrated that, even at the highest surface pressures, a monoglyceride (monopalmitin or monoolein) monolayer is unable to displace completely β-casein molecules from the air−water interface.

Surface Dilatational Characteristics of β-Casein−Monopalmitin Mixed Films at the Air−Water Interface. *The Effect of Surface Pressure.* The surface viscoelastic properties of β-casein−monopalmitin mixed films spread on the air−water interface are shown in **Figure 6**. From the values of the tangent of the loss angle for monopalmitin and β-casein−monopalmitin, it can be concluded that these films behaved as viscoelastic at every surface pressure. For β-casein monolayer tan θ decreased with surface pressure to a low value close to zero. As a consequence of this behavior, it can be established that the surface dilatational characteristics of β-casein monolayers are essentially elastic at the collapse point. In mechanical terms, for proteins forming a close-packed structure at the collapse point the elastic behavior might be attributed to a thin protein gellike layer of collapsed segments at the interface (*18, 20, 31*).

For the β-casein monolayer the $E-\pi$ plot showed an irregular shape. Initially E increased with increasing π to a maximum value at $\pi \cong 10$ mN/m. Upon further increase of the surface pressure E decreased to a minimum at $\pi \cong 20$ mN/m, close to the collapse point. Afterward, E increased again with surface pressure. Other authors observed the same irregular shape in the surface pressure dependence of the surface dilatational
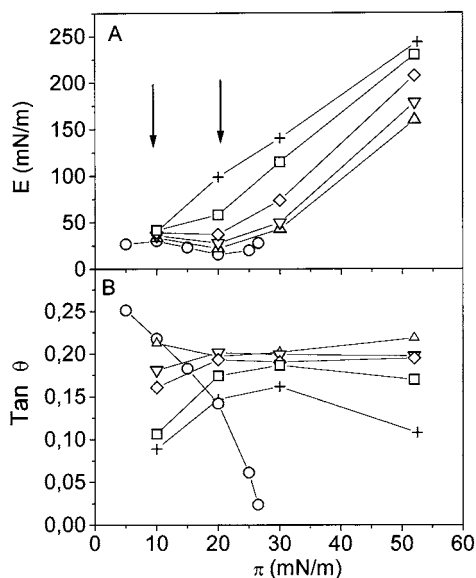
Figure 6. Surface pressure dependence of (A) surface dilatational modulus (E, mN/ m) and (B) loss angle tangent (tan θ) for β-casein–monopalmitin mixed monolayers at 20 °C. Amplitude of the area deformation 5%. Monolayer composition (X_{MP}, w/w %): (○) 0, (△) 0.2, (▽) 0.4, (◇) 0.6, (□) 0.8, and (+) 1. The transitions between the structure **1** and **2** and between the structure **2** and the collapse for a β-casein monolayer are indicated by means of arrows.

modulus for adsorbed (*32*−*34*) and spread (*27*) β-casein films. Interestingly, at these inflection points we also observed the transition between structure 1 and 2 and between structure 2 and monolayer collapse, respectively (**Figure 6**).

For pure monopalmitin monolayer the surface dilatational modulus (**Figure 6A**) also depends on the monolayer structure (**Figure 1**). The more condensed the structure is (at higher π), the higher the surface dilatational modulus of the monolayer becomes until the collapse is reached. The same dependence as with E was observed with the monolayer reflectivity (**Figure 4A**). That is, more condensed monolayer structures may lead to an increase in the interaction forces between the molecules in the interface, which is consistent with the observed increase in E.

For β-casein−monopalmitin mixed films, the surface pressure dependence of E (**Figure 6A**) depends on the surface pressure and the interfacial composition. At surface pressures lower than that for β-casein collapse and at X_{MP} < 0.8, the same irregular shape in the π dependence of E was observed for the mixed films as for pure β-casein. In fact, we have observed the transition between structure **1** and **2** and between structure **2** and monolayer collapse typical for the pure β-casein monolayer also in the mixed films. At surface pressures higher than that for β-casein collapse the $E−\pi$ plot for mixed films were parallel to that for monopalmitin, which demonstrated again that at higher surface pressures the mixed films were practically dominated by monopalmitin molecules. However, the data in **Figure 6A** also demonstrate that the small amounts of β-casein collapsed residues at the interface−as deduced at a microscopic level from $I−\pi$ plots (**Figure 4**) and BAM images (**Figure 5**)− have an effect on the surface dilatational properties of the mixed films. In fact, E for mixed films was lower than for a pure monopalmitin monolayer, even at the collapse point of the mixed films. Thus, the mechanical properties of the mixed films also demonstrated that, even at the highest surface pressure, a monopalmitin monolayer is unable to displace completely β-casein molecules from the air−water interface.
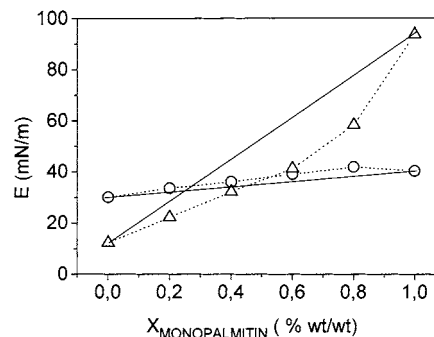

Figure 7. Surface dilatational modulus (**E**) as a function of monolayer composition for β-casein–monopalmitin mixed monolayers. Amplitude of the area deformation 5%. Temperature 20 °C. Surface pressure (○) 10 mN/m and (△) 20 mN/m.

The surface dilational modulus vs interfacial composition is shown in **Figure 7**. It can be seen that the surface dilational modulus of mixed films is similar to or lower than that of an ideal mixture between β-casein and monopalmitin (solid line) at surface pressures lower than or close to the β-casein collapses ($\pi \cong 20.9$ mN/m). These results can been explained if β-casein and monopalmitin molecules are immiscible at the interface, as was deduced from the $\pi−A$ isotherms (**Figures 1**−**3**) and Brewster angle microscopy (**Figures 4** and **5**). The lower E values for mixed films in relation to those for an ideal mixture between β-casein and monopalmitin at surface pressures close to the β-casein collapse may also be associated with the immiscibility between film-forming components and with the displacement of collapsed β-casein by monopalmitin from the interface. As a result of the immiscibility of β-casein and monopalmitin in the mixed film, the interactions between the components are diminished, especially if islands of collapsed β-casein exist at the interface with a variable extension and a random distribution (**Figures 4** and **5**). This phenomenon is in agreement with a reduction in the surface dilational modulus (**Figure 7**) in relation to an ideal mixture of these emulsifiers.

Effect of Frequency. Surface dilational properties for β-casein−monopalmitin mixed monolayers at the collapse point (as an example) are shown, as a function of frequency of oscillation over a range of 1 to 200 mHz, in **Figure 8**. It can be seen that (i) in the range 1 < ω < 50 mHz, the dilational modulus increased with the frequency, but at higher frequencies E is practically constant (**Figure 8A**). (ii) The dilational modulus and its elastic component are essentially the same at frequencies lower than 50 mHz, a phenomenon that explains the low values of tan θ in this region (**Figure 8B**). (iii) Significant differences between both rheological parameters were observed at frequencies higher than 50 mHz. As a consequence of this behavior, the value of tan θ increased with frequency (**Figure 8B**). From these results it can be concluded that monopalmitin monolayers show a rheological behavior under dilational conditions that is essentially elastic at low frequencies (ω < 50) and viscoelastic at higher frequencies (ω > 50). These results are in good agreement with those obtained for pure β-casein adsorbed (*35*) and spread films (*26*) and for monopalmitin under dilational deformation in a ring trough (*36*) and in a Langmuir film balance (*37*).

These findings may be associated with the effect of the rate of deformation on the structure and relaxation phenomena in the monopalmitin area present in the mixed film, because at the collapse point the mixed film is practically dominated by monopalmitin (**Figures 1**, **2**, **4A**, and **5**). For β-casein−monopalmitin mixed monolayers, different relaxation mecha-

Properties of β-Casein–Monoglyceride Mixed Films

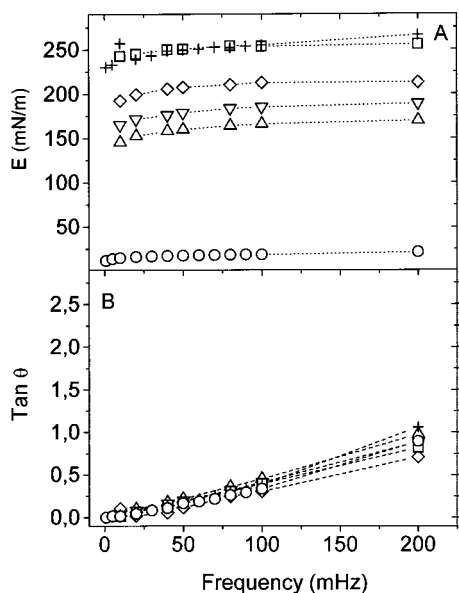*J. Agric. Food Chem.,* Vol. 51, No. 1, 2003 **117**

Figure 8. Frequency dependence of (A) surface dilatational modulus and (B) loss angle tangent for β-casein–monopalmitin mixed monolayers at the collapse point. Temperature: 20 °C. Monolayer composition (X_{MP}, w/w %): (○) 0, (△) 0.2, (▽) 0.4, (◇) 0.6, (□) 0.8, and (+) 1. Amplitude of the area deformation 5%.

nisms may be operative, as a function of surface pressure and the time scale considered, as was discussed in a previous paper (*17*). In fact, the viscoelastic behavior observed for β-casein–monopalmitin monolayers in the frequency range 1−50 mHz should be associated with monopalmitin monolayer collapse. This relaxation process requires a time of the same order of magnitude as the time scale of the oscillation—in our experiments between 1.7 and 16.7 min. Again, the reason for this behavior must be associated with the immiscibility between both components at the air−water interface.

At higher surface frequencies (50 < ω < 200 mHz), the viscoelastic behavior of the mixed monolayer is more complex and should be associated with formation/ destruction of LC domains in monopalmitin coupled with LC-S and LC-LE phase transitions and the formation/destruction of 3-D collapse structures (with the existence of monolayer fractures) (**Figure 5**). We have observed recently by means of long-term relaxation phenomena in β-casein−monopalmitin mixed films (*17*) that the time required for organization/reorganization changes in monopalmitin monolayer structure is of the same order of magnitude as the time scale of the applied deformation.

In **Figures 9** and **10** the results from a sinusoidal deformation for β-casein−monopalmitin mixed films at X_{MP} = 0.2 and X_{MP} = 0.8 and at two frequencies (50 and 200 mHz) are shown. At 50 mHz and at 20 mN/m the LC and LE monopalmitin monolayer structures [MP (LE → LC)] and β-casein with structure **2** [BC (structure **2**)] are constant during the compression−expansion cycles (**Figure 9A**). The results indicate that transition between LE and LC phases and the breaking of intermolecular interactions—mainly between LC domains and, most probably, with change in domain size during the compression−expansion cycles—are both operative in this frequency regime. At the same frequency (50 mHz) and at the collapse point (**Figure 9B**), changes between LC and S structures and between LE and LC phases and a displacement of collapsed β-casein residues, including the formation of multilayers, are produced during the compression−expansion cycles. The same relaxation phenomena, including the overcompression of the
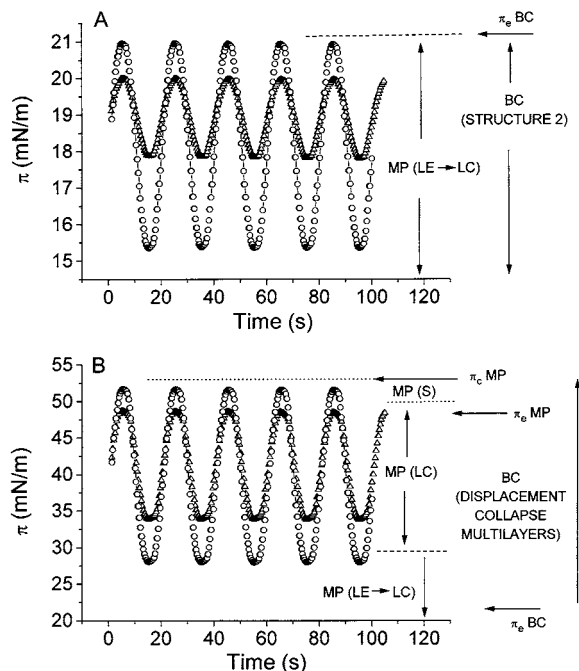

Figure 9. Dynamic surface pressure response to a sinusoidal change in area at a frequency of 50 mHz for β-casein–monopalmitin mixed monolayers at 20 °C. Amplitude of the area deformation 5%. (A) Surface pressure: 20 mN/m. (B) Monolayer collapse point. Monolayer composition (△) X_{MP} = 0.2 and (○) X_{MP} = 0.8. The equilibrium surface pressure for monopalmitin (π_e MP) and β-casein (π_e BC) and the collapse pressure for monopalmitin (π_C MP) are indicated by means of arrows. The transitions between structures and monolayer collapse during sinusoidal compression–expansion cycles for monopalmitin (MP) and β-casein BC) are indicated in the figures.
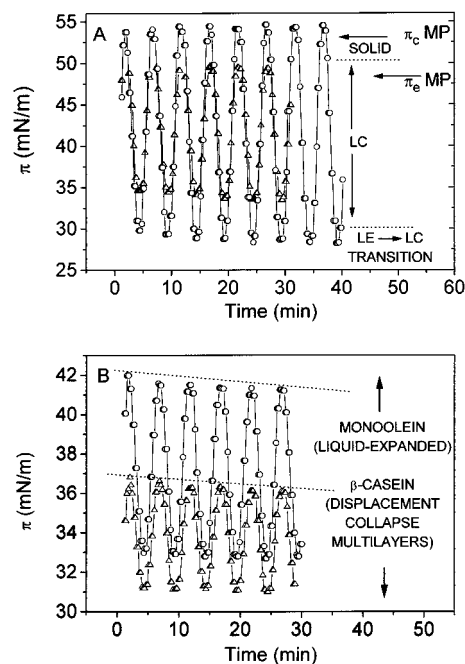

Figure 10. Dynamic surface pressure response to a sinusoidal change in area at a frequency of 200 mHz for (A) β-casein–monopalmitin and (B) β-casein–monoolein mixed monolayers at the collapse point. Temperature 20 °C. Amplitude of the area deformation 5%. Monolayer composition (△) X = 0.2 and (○) X = 0.8.

collapsed monopalmitin monolayer, were observed at a frequency of 200 mHz (**Figure 10A**).
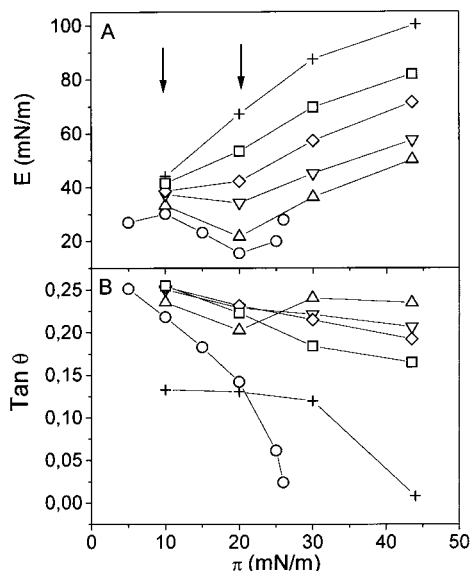
Figure 11. Surface pressure dependence of (A) surface dilatational modulus (E, mN/m) and (B) loss angle tangent (Tan θ) for β-casein-monoolein mixed monolayers at 20 °C. Monolayer composition (X_{MO}, w/w %): (○) 0, (△) 0.2, (▽) 0.4, (◇) 0.6, (□) 0.8, and (+) 1. The transitions between the structure **1** and **2** and between the structure **2** and the collapse for a β-casein monolayer are indicated by means of arrows.

In summary, from the frequency dependence of the surface dilatational properties (E and tan θ) we have elucidated that there exists a close relationship between interfacial dilatational rheology and changes in molecular structure, interactions, miscibility, and relaxation phenomena in the mixed films.

Surface Dilatational Characteristics of β-Casein–Monoolein Mixed Films at the Air–Water Interface. *Effect of Surface Pressure.* As for β-casein–monopalmitin, the values for the surface dilatational properties for β-casein–monoolein monolayers depend on the surface pressure and the monolayer composition (**Figure 11**). Briefly: (i) For pure monoolein monolayer, the more condensed the structure is (at higher π), the higher the surface dilatational modulus of the monolayer becomes before collapse is reached. However, the surface dilatational modulus of monoolein spread monolayer (**Figure 11A**) is lower than that for monopalmitin (**Figure 6A**). The maximum value of E for monoolein is only 40% of that for monopalmitin. The lower collapse pressure in the monoolein film (**Figure 1**) is due to a reduction of the interactions between the molecules in the film (*22, 29*), which could explain the differences in E values between monopalmitin and monoolein at the collapse point. The dilatational modulus is not only determined by the interactions between spread monoglyceride molecules (which depend on the surface pressure), but also the structure of the spread molecule (monopalmitin or monoolein) plays an important role. Thus, for the more condensed monopalmitin monolayer E is higher than for the more expanded monoolein monolayer, at every surface pressure. (ii) At surface pressures lower than that for β-casein collapse and at $X_{MO} <$ 0.8, the same irregular shape in the surface pressure dependence of E (**Figure 11A**) was observed for β-casein and β-casein–monoolein mixed films. (iii) At surface pressures higher than that for β-casein collapse the $E-\pi$ plots for mixed films were parallel to that of monoolein. (iv) The values of E for mixed films are lower than for a pure monoolein monolayer, even at the collapse point of the mixed film. (v) The surface dilatational modulus of mixed films is similar to or lower than that of an ideal mixture between β-casein and monoolein at surface

pressures lower than or close to the β-casein collapse (data not shown). Thus, the same reasoning as used for β-casein–monopalmitin mixed films can be applied here. However, for pure monoolein film at the collapse pressure tan θ is practically zero (**Figure 11B**). This purely elastic behavior may be due to the fact that monoolein collapses with the formation of lenses (*22*).

Effect of Frequency. Surface dilatational properties for β-casein–monoolein mixed monolayers as a function of the frequency of oscillation over a range of 1 to 200 mHz (data not shown) are qualitatively similar to those for β-casein–monopalmitin mixed monolayers (**Figure 8**). However, the effect of the frequency on the relaxation phenomena in β-casein–monoolein mixed films is quite different. At 50 mHz and at 20 mN/m the effect of frequency may be due to loss due to desorption of monoolein (*17, 22*). However, at the collapse point, desorption of monoolein coupled with collapse of the monoolein layer and the displacement and formation of multilayers of collapsed β-casein are the relaxation phenomena likely relevant during the time scale of the compression–expansion cycle (**Figure 10B**). These relaxation phenomena can explain the drift of the baseline with the surface pressure decreasing over a time scale longer than that due to the period of oscillation (**Figure 10B**), which is more significant as the content of monoolein in the mixture increases.

CONCLUSIONS

The static and dynamic characteristics of β-casein and monoglyceride (monopalmitin and monoolein) mixed films depend on the interfacial composition and the surface pressure. At surface pressures lower than that for β-casein collapse, a mixed monolayer of monoglyceride and β-casein may exist. At surface pressures higher than that for β-casein collapse, the mixed monolayers were practically dominated by monoglyceride molecules. The surface dilatational modulus increases as the monolayer is compressed and is a maximum at the highest surface pressures, at the β-casein–monoglyceride collapse point. From the frequency dependence of the surface dilatational properties (E and tan θ) we have elucidated the relationships between interfacial dilatational rheology and changes in molecular structure, interactions, miscibility, and relaxation phenomena.

LITERATURE CITED

(1) Dickinson E. *An Introduction to Food Colloids*; Oxford University Press: Oxford, England, 1992.

(2) Miller, R.; Fainerman, V. B.; Makievski, A. V.; Krägel, J.; Grigoriev, D. O.; Kazakov, V. N.; Sinyachenko, O. V. Dynamics of proteins and mixed protein/surfactant adsorption layers at the air/fluid interface. *Adv. Colloid Interface Sci.* **2000**, *86*, 39–82.

(3) Baszkin, A.; Norde, W. *Physical Chemistry of Biological Interfaces*; Marcel Dekker: New York, 2000.

(4) Becher, P., Ed. *Encyclopedia of Emulsion Technology*; Marcel Dekker: New York, 1985.

(5) Dukhim, S. S.; Kretzschmar, G.; Miller, R. *Dynamic of adsorption at liquid interfaces. Theory, Experiment, Applications*. Elsevier: Amsterdam, 1995.

(6) Malhotra, A. K.; Wasan, D. T. Interfacial rheological properties of adsorbed surfactant films with applications to emulsion and foam stability. *Surfactant Sci. Ser. (Thin Solid Films)* **1988**, *29*, 829–890.

(7) Mittal, K. L.; Kumar, P. *Emulsions, Foams, and Thin Films*. Marcel Dekker: New York, 2000.

(8) de la Fuente, J.; Rodríguez Patino, J. M. Binary mixture of monostearin-distearin monolayers at the air–water interface. *AIChE J.* **1995**, *41*, 1955–1963.

Properties of β-Casein–Monoglyceride Mixed Films

J. Agric. Food Chem., Vol. 51, No. 1, 2003   **119**

(9) de la Fuente, J.; Rodríguez Patino, J. M. Interactions of ethanol in subphase with monostearin-distearin mixed monolayers. *Langmuir* **1995**, *11*, 2163−2172.

(10) de la Fuente, J.; Rodríguez Patino, J. M. Mixed monolayers of acylglycerols on sugar aqueous solutions. *AIChE J.* **1996**, *42*, 1416−1424.

(11) Rodríguez Niño, Mª. R.; Wilde, P. J.; Clark, D. C.; Rodríguez Patino, J. M. Rheokinetic analysis of bovine serum albumin and Tween 20 mixed films on aqueous solutions. *J. Agric. Food Chem.* **1998**, *46*, 2177−2184.

(12) Rodríguez Niño, Mª. R.; Rodríguez Patino, J. M. Surface tension of bovine serum albumin and Tween 20 at the air-aqueous phase interface. *J. Am. Oil Chem. Soc.* **1998**, *75*, 1241−1248.

(13) Rodríguez Patino, J. M.; Carrera, C.; Rodríguez Niño, Mª. R. Analysis of β-casein-monopalmitin mixed films at the air−water interface. *J. Agric. Food Chem.* **1999**, *47*, 4998−5008.

(14) Rodríguez Patino, J. M.; Carrera, C.; Rodríguez Niño, Mª. R. Is Brewster angle microscopy a useful technique to distinguish between isotropic domains in β-casein−monoolein mixed monolayers at the air−water interface? *Langmuir* **1999**, *15*, 4777−4788.

(15) Rodríguez Patino, J. M.; Rodríguez Niño. Mª. R.; Carrera, C.; Cejudo, M. The effect of pH on monoglyceride-caseinate mixed monolayers at the air−water interface. *J. Colloid Interface Sci.* **2001**, *240*, 113−126.

(16) Carrera, C.; de la Fuente, J.; Rodríguez Patino, J. M. Monoglyceride Mixed Films: Structure and Stability". In *Food Colloids*: *Proteins*, *Lipids and Polysaccharides*; Dickinson, E., Bergenstahl, B., Eds.; Royal Society of Chemistry; London, 1997; pp 92−104.

(17) Rodríguez Patino, J. M.; Rodríguez Niño, Mª. R.; Carrera, C. Dynamic properties of β-casein-monoglyceride mixed films at the air−water interface. Long-term relaxation phenomena. *Langmuir* **2002**, *18*, 8455−8463.

(18) Bos, M. A.; van Vliet, T. Interfacial rheological properties of adsorbed protein layers and surfactants: a review. *Adv. Colloid Interface Sci.* **2001**, *91*, 437−471.

(19) Murray, B. S. Interfacial rheology of mixed food proteins and surfactant adsorption layers with respect to emulsion and foam stability. In *Proteins at Liquid Interfaces.* Möbius, D.; Miller, R., Eds.; Elsevier Science BV: Amsterdam, 1998; pp 179−220.

(20) Murray, B. S.; Dickinson, E. Interfacial rheology and the dynamic properties of adsorbed films of food proteins and surfactants. *Food Sci. Technol. Int.* **1996**, *2*, 131−145.

(21) Bos, M. T.; Nylander, T.; Arnebrandt, T.; Clark, D. I. Protein/emulsifier interactions. In *Food emulsifiers and their applications*. Hasenhuette, G. L., Hartel, R. W., Eds.; Chapman & Hall: New York, 1997; pp 95−146.

(22) Carrera, C.; Rodríguez Niño, Mª. R.; Rodríguez Patino, J. M. Relaxation phenomena in monoglyceride films at the air−water interface. *Colloids Surf.*, *B* **1999**, *12*, 175−192.

(23) Rodríguez Niño, Mª. R.; Carrera, S. C.; Rodríguez Patino, J. M. Interfacial characteristics of β-casein films at the air−water interface. *Colloids Surf.*, *B* **1999**, *12*, 161−173.

(24) Rodríguez Patino, J. M.; Carrera, C.; Rodríguez Niño, Mª. R. Morphological and structural characteristics of monoglyceride monolayers at the air−water interface observed by Brewster angle microscopy. *Langmuir* **1999**, *15*, 2484−2492.

(25) Rodríguez Patino, J. M.; Carrera, C.; Rodríguez Niño, Mª. R. Structural and morphological characteristics of β-casein monolayers at the air−water interface. *Food Hydrocolloids* **1999**, *13*, 401−408.

(26) Rodríguez Patino, J. M.; Carrera, S. C.; Rodríguez Niño, Mª. R.; Cejudo, M. Structural-dilatational characteristics relationships of monoglyceride monolayers at the air−water interface. *Langmuir* **2001**, *17*, 4003−4013.

(27) Rodríguez Patino, J. M.; Carrera, S. C.; Rodríguez Niño, Mª. R.; Cejudo, M. Structural and dynamic properties of milk proteins spread at the air−water interface. *J. Colloid Interface Sci.* **2001**, *242*, 141−151.

(28) Lucassen, J.; Van den Tempel, M. Dynamic measurements of dilational properties of a liquid interface. *Chem. Eng. Sci.* **1972**, *27*, 1283−1291.

(29) Graham, D. E.; Phillips, M. C. Proteins at liquid interfaces. III. Molecular structures of adsorbed films. *J. Colloid Interface Sci.* **1979**, *70*, 427−439.

(30) Gaines, G. L. *Insoluble Monolayers at Liquid−Gas Interface.* Wiley: New York, 1966.

(31) Benjamins, J. Static and Dynamic Properties of Proteins Adsorbed at Liquid Interfaces. Ph.D. Thesis, University of Wageningen, The Netherlands, 2000.

(32) Benjamins, J.; Lucassen-Reynders, E. H. Surface dilational rheology of proteins adsorbed at air/water and oil/water interfaces. In *Proteins at Liquid Interfaces*; Möbius, D.; Miller, R., Eds.; Elsevier: Amsterdam, The Netherlands, 1998; pp 341−384.

(33) Gau, C. S.; Yu, H.; Zografi, G. Surface viscoelasticity of β-casein monolayers at the air/water interface by electrocapillary wave diffraction. *J. Colloid Interface Sci.* **1994**, *162*, 214−221.

(34) Lucassen-Reynders, E. H.; Benjamins, J. Dilational rheology of proteins adsorbed at fluid interfaces. In *Food Emulsions and Foams*: *Interfaces*, *Interactions and Stability*. Dickinson, E., Rodríguez Patino, J. M., Eds.; Royal Society of Chemistry: Cambridge, England, 1999; pp 195−206.

(35) Serrien, G.; Geeraerts, G.; Ghosh, L.; Joos, P. Dynamic surface properties of adsorbed protein solutions: BSA, casein and buttermilk. *Colloids Surfaces* **1992**, *68*, 219−233.

(36) Rodríguez Niño, Mª. R.; Wilde, P. J.; Clark, D. C.; Rodríguez Patino, J. M. Surface rheological properties of monostearin and monoolein films spread on the air-aqueous phase interface. *Ind. Eng. Chem. Res.* **1996**, *35*, 4449−4456.

(37) Ruíz, M.; González, I.; Rodríguez Patino, J. M. Aqueous subphase pH influence on nonionizable material monolayers. Structural and rheological characteristics. *Ind. Eng. Chem. Res.* **1998**, *37*, 936−943.